Efficient Numerical Methods for Strongly Anisotropic Elliptic Equations*

Christophe BESSE† Fabrice DELUZET‡ Claudia NEGULESCU§
Chang YANG†¶

February 17, 2012

Abstract

In this paper, we study an efficient numerical scheme for a strongly anisotropic elliptic problem which arises, for example, in the modeling of magnetized plasma dynamics. A small parameter ε induces the anisotropy of the problem and leads to severe numerical difficulties if the problem is solved with standard methods for the case $0 < \varepsilon \ll 1$. An Asymptotic-Preserving scheme is therefore introduced in this paper in a 2D framework, with an anisotropy aligned to one coordinate axis and an ε-intensity which can be either constant or variable within the simulation domain. This AP scheme is uniformly precise in ε, permitting thus the choice of coarse discretization grids, independent of the magnitude of the parameter ε.

Keywords: Anisotropic elliptic equation, singular perturbation model, asymptotic preserving scheme, Scharfetter-Gummel scheme, heterogeneous anisotropy ratios.

1 Introduction

Mathematical study and numerical simulation of highly anisotropic problems are among the most delicate tasks in today's computational science, arising in several fields of

*This work has been supported by the Agence Nationale de la Recherche (ANR) under contract IODISSEE (ANR-09-COSI-007-02). The first two authors would like to express their gratitude to G. Gallice and C. Tessieras from CEA-Cesta for bringing their attention to this problem.
All the authors would like to acknowledge Pierre Degond for fruitful discussions and his help for improving this paper.

†Laboratoire Paul Painlevé (UMR 8524), Université Lille 1, cité scientifique, 59655 Villeneuve d'Ascq Cedex, France. (christophe.besse@math.univ-lille1.fr, chang.yang@math.univ-lille1.fr)

‡Université de Toulouse, UPS, INSA, UT1, UTM, Institut de Mathématiques de Toulouse, F-31062 Toulouse, France; CNRS, Institut de Mathématiques de Toulouse UMR 5219, F-31062 Toulouse, France. (fabrice.deluzet@math.univ-toulouse.fr)

§CMI/LATP (UMR 6632), université de Provence; 39, rue Joliot Curie; 13453 Marseille Cedex, France. (claudia.negulescu@cmi.univ-mrs.fr)

¶Corresponding author

applications. Examples are flows in porous media [2, 10], semiconductor modeling [16], quasi-neutral plasma simulations [5], image processing [24, 25], atmospheric or oceanic flows [22], the list of possible applications being not exhaustive. The motivation of this work is closely related to the magnetized plasma simulations such as atmospheric plasmas [8, 11, 13, 14, 17].

The difficulties encountered when trying to solve numerically such problems, come from the occurring severe anisotropy. Indeed, the anisotropy requires (for precise results) the use of grids which have to be refined in order to compensate the anisotropy, this procedure being definitively too expensive for large anisotropy ratios. The aim of the present paper is to introduce an efficient numerical scheme for an accurate resolution of such type of problems, without restrictions on the discretization meshes.

To perceive these numerical difficulties, let us present a 2D model containing these problems which was already studied in [6]. A generalization to 3D geometries is straightforward. The anisotropy is considered in the present study, to be aligned with the z-direction. For simplicity reasons, let $\Omega = \Omega_x \times \Omega_z$ where $\Omega_x \subset \mathbb{R}$ and $\Omega_z \subset \mathbb{R}$ are intervals. The investigated 2D singular perturbation elliptic problem writes

$$\begin{cases} -\nabla \cdot (\mathcal{A} \nabla \phi^\varepsilon) = f, & \text{in } \Omega, \\ \phi^\varepsilon = 0, \text{ on } \partial\Omega_x \times \Omega_z, & \partial_z \phi^\varepsilon = 0, \text{ on } \Omega_x \times \partial\Omega_z, \end{cases} \tag{1.1}$$

where the diffusion matrix $\mathcal{A}$ is defined by

$$\mathcal{A} = \begin{pmatrix} A_\perp & 0 \\ 0 & \frac{1}{\varepsilon} A_z \end{pmatrix} \tag{1.2}$$

and $A_\perp(x,z)$ and $A_z(x,z)$ are known functions of the same order of magnitude, while the parameter $0 < \varepsilon \leq 1$ may be very small, thus provoking the anisotropy of the problem. Problem (1.1) is a typical singular perturbation problem (SP-model) and can be rewritten as follows

$$(\mathrm{SP}) \begin{cases} -\dfrac{\partial}{\partial x}\left(\varepsilon A_\perp \dfrac{\partial \phi^\varepsilon}{\partial x}\right) - \dfrac{\partial}{\partial z}\left(A_z \dfrac{\partial \phi^\varepsilon}{\partial z}\right) = \varepsilon f, & \text{in } \Omega, \\ \phi^\varepsilon = 0, & \text{on } \partial\Omega_x \times \Omega_z, \\ \partial_z \phi^\varepsilon = 0, & \text{on } \Omega_x \times \partial\Omega_z. \end{cases} \tag{1.3}$$

This model is a well-posed boundary value problem which has a unique solution for all fixed $\varepsilon > 0$. However, setting formally $\varepsilon = 0$ in this equation, we obtain a degenerate problem reading:

$$\begin{cases} -\dfrac{\partial}{\partial z}\left(A_z \dfrac{\partial \psi}{\partial z}\right) = 0, & \text{in } \Omega, \\ \psi = 0, & \text{on } \partial\Omega_x \times \Omega_z, \\ \partial_z \psi = 0, & \text{on } \Omega_x \times \partial\Omega_z. \end{cases} \tag{1.4}$$

The model (1.4) is ill-posed due to the loss of uniqueness of the solution. Indeed, all the functions ψ depending only on the x-coordinate and verifying the boundary condition $\psi = 0$ on $\partial\Omega_x$ satisfy (1.4). This ill-posedness is the reason why standard methods, discretizing the singular perturbation problem (1.3), are not adapted for computations

with $\varepsilon \ll 1$, requiring a grid mesh dependent on ε in order to get accurate results. But mesh refinement leads necessarily to high numerical costs and memory usage as well as limited anisotropy ratios, hence the need of more performant methods.

We would like to remark here, that the choice of the boundary conditions is guided by the physics. The numerical difficulties encountered in this work are closely related to the fact that the dominant operator is supplied with Neumann boundary conditions. The same difficulty exists for periodic boundary conditions. Contrariwise, Dirichlet boundary conditions would lead to a well-posed problem, when setting $\varepsilon = 0$.

We have seen that the formal limit of the SP-problem is ill-posed, leading to numerical difficulties. However, what can be observed is that the sequence $(\phi^\varepsilon)_\varepsilon$, ϕ^ε being the solution of the SP-model (1.3) for $\varepsilon > 0$, is converging for $\varepsilon \to 0$ towards a limit function ϕ^0, which is the unique solution of a well-posed problem, called in the sequel L-problem (Limit problem). To identify this limit problem, let us define the mean value $\overline{f}$ of the function f along the anisotropy direction, *i.e.*

$$\overline{f}(x) = \frac{1}{\mathrm{mes}(\Omega_z)} \int_{\Omega_z} f(x,z)\, dz\,, \qquad \forall x \in \Omega_x\,.$$

Then the L-problem writes

$$(\mathrm{L}) \left\{ \begin{array}{ll} -\dfrac{\partial}{\partial x}\left(\overline{A}_\perp \dfrac{\partial \phi^0}{\partial x}\right) = \overline{f}, & \text{in } \Omega_x\,, \\ \phi^0 = 0\,, & \text{on } \partial\Omega_x\,. \end{array} \right. \tag{1.5}$$

To capture numerically this limit problem when $\varepsilon \ll 1$, an asymptotic preserving scheme was introduced in [6]. Initially, AP-schemes were introduced by S. Jin [12] for the study of multi-scale kinetic equations. The main idea of the obtention of AP-schemes relies on a reformulation of the singular perturbation (SP) problem into an equivalent set of equations for which the limit $\varepsilon \to 0$ is regular. In this aim, the paper [6] proposes a reformulation, in which, the solution is decomposed into a mean value, accordingly to the anisotropy ($z-$) direction, corrected by a fluctuation. This reformulation reduces in the limit $\varepsilon \to 0$ towards the well-posed limit model (1.5). The efficiency of this AP-scheme was proved in [6], in particular its uniform convergence with respect to ε.

In the present paper, we want to introduce some essential improvements of the initial AP-scheme. The objective of these improvements and developments is, on one hand, to enhance the numerical efficiency of the method, and on the other hand, to extend this scheme to more realistic physical problems, namely variable ε intensities.

The new reformulation still relies on a decomposition of the solution in a fluctuating and a mean part, however, in this new approach, the system for the fluctuation is different and much sparser than that of the previous formulation, increasing thus considerably the numerical efficiency (reduced computational time and memory usage as illustrated by Figure 1). A direct method is used, in the present paper, for the resolution of the obtained sparse linear system, in contrast to the iterative resolution proposed in [6]. This direct method is shown to be more efficient for the numerical experiments investigated.

Furthermore, in the present paper we are also interested in variable anisotropy ratios in view of real physical configurations. For some applications (for instance ionospheric

plasma physics) large variations and steep gradients can be observed in this ratio. This feature has motivated the adaptation of our new AP-scheme to highly heterogeneous anisotropies. With this procedure, one can avoid in particular the use of hybrid methods, which are quite challenging from a practical point of view. To improve the accuracy of the scheme in this framework, a Scharfetter-Gummel [21] version of the method is proposed and compared to standard quadrature formulae. The thus obtained new AP scheme permits to address, in a simple way, real physical simulations without too long computational times.

Let us remark that a different approach is presented in [7] in the aim to solve similar anisotropic elliptic problems. The AP reformulation proposed there is based on a different decomposition of the unknown function ϕ (micro-macro decomposition), which permits to avoid the introduction of Lagrange multipliers, keeping thus the number of unknowns reduced. These Lagrange multipliers are essential in the here proposed AP-version, in order to take into account for the zero mean constraint of the fluctuation part (see section 2). The advantage of the present approach is that it allows a straightforward implementation of the AP-scheme, starting from a standard discretization of the problem (1.3–1.2).

This paper is organized as follows: in section 2, we introduce the new AP-reformulation as well as its weak formulation. The existence and uniqueness of the reformulated continuous and discrete system solutions are studied. A $\mathbb{Q}_1$ finite element method is used to discretize the problem, and the numerical results are investigated for values of ε below the computer arithmetic precision. In section 3, the AP scheme is extended to the variable ε-case, with large gradients. Finally, discretizations and numerical results are presented and analyzed.

2 Derivation of a new asymptotic preserving scheme for a uniform anisotropy ratio ε

In this section, a new Asymptotic Preserving reformulation is introduced for the singularly perturbed problem (1.3) in a framework comparable to that of the previous study [6], *i.e.* we are considering the constant ε case. The advantages of this new AP scheme as compared with the original one (presented in [6]) shall be outlined here.

The present section is organized as follows. The new AP formulation is stated in subsection 2.1. Subsection 2.2 is concerned with mathematical investigations, in particular existence and uniqueness of solutions. The numerical discretization is briefly detailed in subsection 2.3, before carrying out the numerical experiments .

2.1 Asymptotic preserving formulation

The main idea of the Asymptotic Preserving method introduced in [6] is to decompose the singular perturbation solution ϕ^ε into two parts: $\overline{\phi^\varepsilon}$, the mean part integrated along the z-axis, complemented with the fluctuating part $(\phi^\varepsilon)'$ defined by $(\phi^\varepsilon)' = \phi^\varepsilon - \overline{\phi^\varepsilon}$. With these new unknowns, the system (1.3) is decomposed into respectively an average equation for $\overline{\phi^\varepsilon}$ and a fluctuation equation for $(\phi^\varepsilon)'$. The average equation is very similar to the limit problem (1.5) and provides an accurate manner for computing the mean

part for all $\varepsilon > 0$. Moreover, the fluctuating part satisfies $\overline{(\phi^\varepsilon)'} = 0$, which is the fundamental property in deriving the AP scheme, and in particular which shall permit to get an accuracy independent of ε-values. Let us detail now more precisely all these steps.

We shall assume in the sequel the following hypothesis.

Hypothesis 1. *Let the diffusion functions $A_\perp \in L^\infty(\Omega)$ and $A_z \in L^\infty(\Omega)$ satisfy $0 < c_\perp \leq A_\perp(x,z) \leq M_\perp$, $0 < c_z \leq A_z(x,z) \leq M_z$, where $c_\perp$, c_z, $M_\perp$ and M_z are some positive constants. Moreover let $f \in L^2(\Omega)$.*

For the sake of simplicity, let $\Omega_x = [0, L_x]$ and $\Omega_z = [0, L_z]$ and let us omit the ε-index of the solution ϕ^ε whenever there is no confusion. There are some useful properties of the average and fluctuation operations, listed below

$$\overline{f'} = 0, \ \overline{fg} = \bar{f}\bar{g} + \overline{f'g'}, \ \overline{f'g'} = \overline{f'g} = \overline{fg'}, \tag{2.1}$$

$$\overline{\frac{\partial f}{\partial x}} = \frac{\partial \bar{f}}{\partial x}, \ \frac{\partial f}{\partial z} = \frac{\partial f'}{\partial z}, \ \left(\frac{\partial f}{\partial x}\right)' = \frac{\partial f'}{\partial x}, \tag{2.2}$$

$$(fg)' = f'g' - \overline{f'g'} + \bar{f}g' + f'\bar{g}. \tag{2.3}$$

By taking now the average of the equation (1.3) along the z-axis and by considering the properties (2.1), the equation for the mean part of the solution writes:

$$\begin{cases} -\dfrac{\partial}{\partial x}\left(\overline{A_\perp}\dfrac{\partial \bar{\phi}}{\partial x}\right) = \bar{f} + \dfrac{\partial}{\partial x}\left(\overline{A_\perp \dfrac{\partial \phi'}{\partial x}}\right), & \text{in } \Omega_x, \\ \bar{\phi} = 0, & \text{on } \partial\Omega_x. \end{cases} \tag{2.4}$$

The equation for the fluctuating part, proposed in this paper, is straightforwardly derived by introducing the decomposition $\phi(x,z) = \phi'(x,z) + \bar{\phi}(x)$ in (1.3) and by applying (2.2), yielding thus

$$\begin{cases} -\varepsilon\dfrac{\partial}{\partial x}\left(A_\perp\dfrac{\partial \phi'}{\partial x}\right) - \dfrac{\partial}{\partial z}\left(A_z\dfrac{\partial \phi'}{\partial z}\right) = \varepsilon f + \varepsilon\dfrac{\partial}{\partial x}\left(A_\perp\dfrac{\partial \bar{\phi}}{\partial x}\right), & \text{in } \Omega, \\ \phi' = 0, & \text{on } \partial\Omega_x \times \Omega_z, \\ \partial_z \phi' = 0, & \text{on } \Omega_x \times \partial\Omega_z, \\ \overline{\phi'} = 0, & \text{in } \Omega_x. \end{cases} \tag{2.5}$$

The system (2.4),(2.5) will be referred to as the new AP-formulation. It differs from the one introduced in the original paper [6] by the equation for the fluctuating part, whose derivation is briefly detailed here for comparison purpose. By subtracting the average

equation (2.4) from (1.3) and by using (2.3), one gets the different fluctuation system

$$\begin{cases} -\varepsilon\dfrac{\partial}{\partial x}\left(A_\perp\dfrac{\partial\phi'}{\partial x}\right)-\dfrac{\partial}{\partial z}\left(A_z\dfrac{\partial\phi'}{\partial z}\right)+\varepsilon\dfrac{\partial}{\partial x}\left(\overline{A'_\perp\dfrac{\partial\phi'}{\partial x}}\right)= & \\ \qquad\qquad\varepsilon f'+\varepsilon\dfrac{\partial}{\partial x}\left(A'_\perp\dfrac{\partial\bar{\phi}}{\partial x}\right), & \text{in } \Omega, \\ \phi'=0, & \text{on } \partial\Omega_x\times\Omega_z, \\ \partial_z\phi'=0, & \text{on } \Omega_x\times\partial\Omega_z, \\ \overline{\phi'}=0, & \text{in } \Omega_x. \end{cases} \tag{2.6}$$

The coupled system (2.4),(2.6) was introduced and analyzed in [6]. The two reformulation (2.4),(2.5) resp. (2.4),(2.6) are equivalent. We investigate below their asymptotic preserving properties and their ability to provide a precise computation of the solution of (1.3) for all values of ε.

First note that, for given $\phi' \in H^1(\Omega)$ the average equation (2.4) is a well-posed boundary value problem, which is independent of ε. Moreover, letting $\varepsilon \to 0$ in the fluctuation equation (2.5) or (2.6), yields

$$\begin{cases} -\dfrac{\partial}{\partial z}\left(A_z\dfrac{\partial\phi'}{\partial z}\right)=0, & \text{in } \Omega, \\ \phi'=0, & \text{on } \partial\Omega_x\times\Omega_z, \\ \partial_z\phi'=0, & \text{on } \Omega_x\times\partial\Omega_z, \\ \overline{\phi'}=0, & \text{in } \Omega_x. \end{cases} \tag{2.7}$$

In contrast to (1.4), this problem is well-posed with a unique solution $\phi' \equiv 0$. Indeed, it is the constraint $\overline{\phi'}=0$ which implies the uniqueness of the solution. And it is also this property of zero mean value for the fluctuating part ϕ' in (2.5) resp. (2.6), which provides an equation with a condition number independent of the ε-values.

Now, setting $\phi'=0$ into the average equation (2.4), yields the limit model (1.5). This demonstrates that the reformulated systems (2.4),(2.5) resp. (2.4),(2.6) are regular perturbations of the L-model for $\varepsilon \to 0$.

The equation (2.6) for the fluctuating part ϕ' has been designed in [6] in order to have a zero mean value right hand-side, thus ensuring that the fluctuating part itself satisfies this property automatically for $\varepsilon > 0$ and justifying by this manner the introduction of the crucial constraint $\overline{\phi'}=0$. However this fluctuation equation incorporates a term, namely $\frac{\partial}{\partial x}\left(\overline{A'_\perp\frac{\partial\phi'}{\partial x}}\right)$, which fills the matrix in the discretization step. For this reason, this paper will focus on the sparse alternative (2.4),(2.5), more efficient in terms of numerical memory usage and computations (as illustrated in Figure 1). Due to the equivalence of the two AP-formulations, one has the important property $\overline{\phi'}\equiv 0$ even in system (2.4),(2.5), although the right hand-side of (2.5) does not satisfy this zero mean value property.

Note that for both formulations, the equations providing the mean and the fluctuating parts are coupled. Two strategies can be proposed in order to solve this coupled system: an iterative one, suggested in [6], performing a successive resolution of (2.4),(2.5) starting from some initial guess ϕ', or a direct resolution adopted in this paper.

2.2 Weak formulation

In order to introduce the weak form of the AP scheme (2.4),(2.5), let us introduce two Hilbert-spaces

$$\mathbb{V} = \{\psi(x,z) \in H^1(\Omega)/\psi = 0 \text{ on } \partial\Omega_x \times \Omega_z\},\ \mathbb{W} = \{\bar{\psi}(x) \in H^1(\Omega_x)/\bar{\psi} = 0 \text{ on } \partial\Omega_x\},$$

and the corresponding scalar products

$$(\phi,\psi)_{\mathbb{V}} = \varepsilon(\partial_x\phi, \partial_x\psi)_{L^2(\Omega)} + (\partial_z\phi, \partial_z\psi)_{L^2(\Omega)},\ (\bar{\phi},\bar{\psi})_{\mathbb{W}} = (\partial_x\bar{\phi}, \partial_x\bar{\psi})_{L^2(\Omega_x)}.$$

For simplicity, we denote in the sequel the L^2 scalar-product simply by the bracket $(\cdot,\cdot)$. By defining the following bilinear forms

$$\begin{aligned}
a_0(\phi',\psi') &:= \int_0^{Lz}\int_0^{Lx} A_z(x,z)\frac{\partial\phi'}{\partial z}(x,z)\frac{\partial\psi'}{\partial z}(x,z)dxdz, \quad \forall(\phi',\psi') \in \mathbb{V}^2\\
a_1(\phi',\psi') &:= \int_0^{Lz}\int_0^{Lx} A_\perp(x,z)\frac{\partial\phi'}{\partial x}(x,z)\frac{\partial\psi'}{\partial x}(x,z)dxdz, \quad \forall(\phi',\psi') \in \mathbb{V}^2\\
a_2(\bar{\phi},\bar{\psi}) &:= \int_0^{Lx} \bar{A}_\perp(x)\frac{\partial\bar{\phi}}{\partial x}(x)\frac{\partial\bar{\psi}}{\partial x}(x)dx, \quad \forall(\bar{\phi},\bar{\psi}) \in \mathbb{W}^2\\
a(\phi',\psi') &:= a_0(\phi',\psi') + \varepsilon a_1(\phi',\psi'), \quad \forall(\phi',\psi') \in \mathbb{V}^2\\
b(\bar{P},\psi') &:= \int_0^{Lx} \bar{P}(x)\int_0^{Lz}\psi'(x,z)dz\,dx \quad \forall(\bar{P},\psi') \in L^2(\Omega_x)\times L^2(\Omega)\,.\\
c(\bar{\phi},\psi') &:= \int_0^{Lz}\int_0^{Lx} A_\perp(x,z)\frac{\partial\bar{\phi}}{\partial x}(x)\frac{\partial\psi'}{\partial x}(x,z)dxdz, \quad \forall(\bar{\phi},\psi') \in \mathbb{W}\times\mathbb{V}
\end{aligned} \tag{2.8}$$

we can write the weak formulations of the SP-model resp. L-model as follows: Find $\phi^\varepsilon \in \mathbb{V}$ resp. $\phi^0 \in \mathbb{W}$, solution of

$$\text{(SP)} \qquad \varepsilon a_1(\phi^\varepsilon,\psi) + a_0(\phi^\varepsilon,\psi) = \varepsilon(f,\psi),\ \forall\psi \in \mathbb{V}, \tag{2.9}$$

$$\text{(L)} \qquad a_2(\phi^0,\psi^0) = (\bar{f},\psi^0),\ \forall\psi^0 \in \mathbb{W}. \tag{2.10}$$

Introducing in (SP) the decomposition $\phi^\varepsilon = \overline{\phi^\varepsilon} + (\phi^\varepsilon)'$ and taking test-functions $\psi' \in \mathbb{V}$ resp. $\bar{\psi} \in \mathbb{W}$ give rise to the following equivalent reformulation of the SP-model

$$\begin{cases} a_2(\overline{\phi^\varepsilon},\bar{\psi}) = (\bar{f},\bar{\psi}) - \frac{1}{L_z}c(\bar{\psi},(\phi^\varepsilon)'), \quad \forall\bar{\psi} \in \mathbb{W},\\ a((\phi^\varepsilon)',\psi') = \varepsilon(f,\psi') - \varepsilon c(\overline{\phi^\varepsilon},\psi'), \quad \forall\psi' \in \mathbb{V}. \end{cases} \tag{2.11}$$

In order to remain well-posed even in the limit of $\varepsilon \to 0$, we have to introduce the constraint $\overline{(\phi^\varepsilon)'} \equiv 0$ into the fluctuation equation as mentioned in subsection 2.1.

This is realized via the introduction of a Lagrange multiplier $\bar{P}$ [6] as follows : Find $(\overline{\phi^\varepsilon}, (\phi^\varepsilon)', \overline{P^\varepsilon}) \in \mathbb{W} \times \mathbb{V} \times L^2(\Omega_x)$, solution of

$$(AP) \begin{cases} a_2(\overline{\phi^\varepsilon}, \bar{\psi}) = (\bar{f}, \bar{\psi}) - \frac{1}{L_z} c(\bar{\psi}, (\phi^\varepsilon)'), & \forall \bar{\psi} \in \mathbb{W}, \quad (a) \\ a((\phi^\varepsilon)', \psi') + b(\bar{P}, \psi') = \varepsilon(f, \psi') - \varepsilon c(\overline{\phi^\varepsilon}, \psi'), & \forall \psi' \in \mathbb{V}, \quad (b) \\ b(\bar{Q}, (\phi^\varepsilon)') = 0, & \forall \bar{Q} \in L^2(\Omega_x). \quad (c) \end{cases} \tag{2.12}$$

This system will be called in the sequel the AP-formulation of the SP-model. The next theorem proves the well-posedness of the AP-formulation (2.12) for fixed $\varepsilon > 0$, the equivalence with problem (2.11) and analyzes the convergence of the solution $(\overline{\phi^\varepsilon}, (\phi^\varepsilon)') \in \mathbb{W} \times \mathbb{V}$. In particular it shows also that the AP scheme is well-posed even in the limit $\varepsilon \to 0$.

Theorem 2.1. *Under hypothesis 1, for all fixed $\varepsilon > 0$, there exists a unique solution $(\overline{\phi^\varepsilon}, (\phi^\varepsilon)', \overline{P^\varepsilon}) \in \mathbb{W} \times \mathbb{V} \times L^2(\Omega_x)$ satisfying (2.12). The function $\phi^\varepsilon = \overline{\phi^\varepsilon} + (\phi^\varepsilon)'$ is the unique solution of (2.9). Furthermore, the system (2.11) is equivalent to the system (2.12), which means $(\overline{\phi^\varepsilon}, (\phi^\varepsilon)') \in \mathbb{W} \times \mathbb{V}$ is the unique solution of (2.11) if and only if $(\overline{\phi^\varepsilon}, (\phi^\varepsilon)', \overline{P^\varepsilon}) \in \mathbb{W} \times \mathbb{V} \times L^2(\Omega_x)$ is the unique solution of (2.12), with $\overline{P^\varepsilon} \equiv 0$. Finally, in the limit $\varepsilon \to 0$, the pair $(\overline{\phi^\varepsilon}, (\phi^\varepsilon)')$ converges strongly towards some function $(\overline{\phi^0}, (\phi^0)') \in \mathbb{W} \times \mathbb{V}$, where $\overline{\phi^0}$ is the unique weak solution of the L-model and $(\phi^0)' \equiv 0$.*

Proof. This theorem was proven in [6] for the system (2.4),(2.6). Using the equivalence between the AP-formulation of [6] (2.4),(2.6) and the present one (2.4),(2.5), one can immediately adapt the proof.

□

Remark that if we ask more regularity of the coefficients $A_\perp$ and A_z, then we can obtain a more regular solution of the SP-model (1.3). This is a simple regularity result for elliptic equations.

Hypothesis 2. *Let the diffusion functions $A_\perp \in W^{1,\infty}(\Omega)$ and $A_z \in W^{1,\infty}(\Omega)$ satisfy $0 < c_\perp \leq A_\perp(x,z) \leq M_\perp$, $0 < c_z \leq A_z(x,z) \leq M_z$, where $c_\perp$, c_z, $M_\perp$ and M_z are some positive constants. Moreover let $f \in L^2(\Omega)$.*

Lemma 2.2. *Under hypothesis 2, for all fixed $\varepsilon > 0$ there exists a unique solution of the SP-model (1.3), satisfying $\phi \in \mathbb{V} \cap H^2(\Omega)$. Furthermore, the statement of Theorem 2.1 holds by replacing $\mathbb{V}$ resp. $\mathbb{W}$ by $\mathbb{V} \cap H^2(\Omega)$ resp. $\mathbb{W} \cap H^2(\Omega_x)$.*

2.3 Numerical methods and experiments

The aim of this section shall be to introduce a numerical discretization of the AP-formulation (2.12), to investigate the existence and uniqueness of discrete solutions and to analyze the obtained results.

2.3.1 A finite element discretization

To discretize system (2.12), we introduce the homogeneous partitions, *i.e.* $x_i = i\Delta x$, $i = 0, \dots, N_x + 1$, and $z_k = k\Delta z$, $k = 0, \dots, N_z + 1$, and the finite element $\mathbb{P}_1$ hat functions

$$\chi_i(x) = \begin{cases} \frac{x - x_{i-1}}{\Delta x}, & x \in [x_{i-1}, x_i), \\ \frac{x_{i+1} - x}{\Delta x}, & x \in [x_i, x_{i+1}), \\ 0, & \text{else}, \end{cases}, \qquad i = 1, \cdots, N_x,$$

$$\kappa_k(z) = \begin{cases} \frac{z - z_{k-1}}{\Delta z}, & z \in [z_{k-1}, z_k), \\ \frac{z_{k+1} - z}{\Delta z}, & z \in [z_k, z_{k+1}), \\ 0, & \text{else}, \end{cases}, \qquad k = 1, \cdots, N_z,$$

$$\kappa_0(z) = \begin{cases} \frac{z_1 - z}{\Delta z}, & z \in [z_0, z_1), \\ 0, & \text{else}, \end{cases}, \qquad \kappa_{N_z+1}(z) = \begin{cases} \frac{z - z_{N_z}}{\Delta z}, & z \in [z_{N_z}, z_{N_z+1}), \\ 0, & \text{else}. \end{cases}$$

Note that in a Cartesian mesh the tensor product of $\mathbb{P}_1$ hat functions χ_i and κ_k coincides with $\mathbb{Q}_1$ finite element basis functions. The discrete spaces $\mathbb{V}_h \subset \mathbb{V}$, $\mathbb{W}_h \subset \mathbb{W}$ and $\mathbb{L}_h \subset L^2(\Omega_x)$ are generated respectively via the basis functions $(\chi_i)_{i=1,\dots,N_x}$ and $(\kappa_k)_{k=0,\dots,N_z+1}$.

Thus we can write the approximations of the unknowns $\phi'_h \in \mathbb{V}_h$, $\bar{\phi}_h \in \mathbb{W}_h$, $\bar{P}_h \in \mathbb{L}_h$ in the form

$$\phi'_h(x,z) = \sum_{i=1}^{N_x} \sum_{k=0}^{N_z+1} \alpha_{ik} \chi_i(x) \kappa_k(z), \ \bar{\phi}_h(x) = \sum_{i=1}^{N_x} \beta_i \chi_i(x), \ \bar{P}_h(x) = \sum_{i=1}^{N_x} \gamma_i \chi_i(x). \tag{2.13}$$

The discretized AP scheme can now be expressed as follows: Find $(\overline{\phi_h}, \phi'_h, \overline{P}_h) \in \mathbb{W}_h \times \mathbb{V}_h \times \mathbb{L}_h$ solution of

$$(AP)_h \begin{cases} a_2(\bar{\phi}_h, \bar{\psi}_h) = (\bar{f}, \bar{\psi}_h) - \frac{1}{L_z} c(\bar{\psi}_h, \phi'_h), & \forall \bar{\psi}_h \in \mathbb{W}_h, \\ a(\phi'_h, \psi'_h) + b(\bar{P}_h, \psi'_h) = \varepsilon(f, \psi'_h) - \varepsilon c(\bar{\phi}_h, \psi'_h), & \forall \psi'_h \in \mathbb{V}_h, \\ b(\bar{Q}_h, \phi'_h) = 0, & \forall \bar{Q}_h \in \mathbb{L}_h. \end{cases} \tag{2.14}$$

Denoting by $A_2 \in \mathbb{R}^{N_x \times N_x}$, $A \in \mathbb{R}^{N_x(N_z+2) \times N_x(N_z+2)}$, $B, C \in \mathbb{R}^{N_x \times N_x(N_z+2)}$ the matrices associated with the bilinear forms a_2, a, b, c respectively and moreover let us define the right-hand sides $F_1 \in \mathbb{R}^{N_x(N_z+2)}$, $F_2 \in \mathbb{R}^{N_x}$ by

$$F_1(ik) := \varepsilon(f, \chi_i \kappa_k), \quad F_2(i) := (\bar{f}, \chi_i), \qquad \forall i = 1, \dots, N_x, \, k = 0, \dots, N_z + 1,$$

then the discrete system can then be recasted in : Find $(\alpha, \beta, \gamma) \in \mathbb{R}^{N_x(N_z+2)} \times \mathbb{R}^{N_x} \times \mathbb{R}^{N_x}$ solution of

$$\begin{pmatrix} A & \varepsilon C & B \\ \frac{1}{L_z} C^T & A_2 & 0 \\ B^T & 0 & 0 \end{pmatrix} \begin{pmatrix} \alpha \\ \beta \\ \gamma \end{pmatrix} = \begin{pmatrix} F_1 \\ F_2 \\ 0 \end{pmatrix}. \tag{2.15}$$

In the present paper, we shall solve the system (2.15) directly with an appropriate linear solver. Moreover, following an idea proposed in [6] to treat (2.4),(2.6), we propose the following decoupling

$$A_2\beta^{(n+1)} = F_2 - \frac{1}{L_z}C^T\alpha^{(n)}\,, \tag{2.16a}$$

$$\begin{pmatrix} A & B \\ B^T & 0 \end{pmatrix}\begin{pmatrix} \alpha^{(n+1)} \\ \gamma^{(n+1)} \end{pmatrix} = \begin{pmatrix} F_1 \\ 0 \end{pmatrix} - \begin{pmatrix} 0 & \varepsilon C \\ 0 & 0 \end{pmatrix}\begin{pmatrix} 0 \\ \beta^{(n+1)} \end{pmatrix}. \tag{2.16b}$$

We denote this method as iterative AP scheme in the sequel, which consists in solving the equation for the mean part using an estimation of the fluctuating part, and then to compute a better estimate of the fluctuating part thanks to the updated mean approximation. We shall compare, in our numerical studies, these two resolution procedures.

Let us prove now, that the discrete AP-formulation (2.14) has also a unique solution, in other words, that the linear system (2.15) is invertible.

Theorem 2.3. *Let $\varepsilon > 0$ be fixed and let us suppose that hypothesis 1 is satisfied. Then the discrete AP-formulation (2.14) admits a unique solution $(\overline{\phi_h}, \phi_h', \overline{P}_h) \in \mathbb{W}_h \times \mathbb{V}_h \times \mathbb{L}_h$.*

Proof. As we consider now a finite dimensional linear system, we have only to check the uniqueness of the solution. For this, let $f \equiv 0$ and let us show that this implies $(\overline{\phi_h}, \phi_h', \overline{P}_h) \equiv 0$. The proof is very similar to the proof of the uniqueness of the solution in the continuous case.

The first step is to show that $\overline{P}_h = 0$. For this let us take in the second equation of (2.14) test functions $\psi_h' \in \mathbb{W}_h$ depending only on the x-coordinate. By using the first equation, this implies $b(\bar{P}_h, \psi_h') = 0$ for all $\psi_h' \in \mathbb{W}_h$, yielding immediately $\overline{P}_h = 0$.
The second step is to show that $(\overline{\phi_h}, \phi_h') \equiv (0,0)$. For this, let us take in the second equation of (2.14) a test function $\psi_h' := \overline{\phi_h} + \phi_h' \in \mathbb{V}_h$. This yields

$$\int_0^{L_x}\int_0^{L_z} A_z|\partial_z\phi_h'|^2 dzdx + \varepsilon\int_0^{L_x}\int_0^{L_z} A_\perp|\partial_x(\phi_h' + \overline{\phi_h})|^2 dzdx = 0\,,$$

implying thus $\overline{\phi_h} + \phi_h' \equiv cst$. Due to the Dirichlet boundary conditions, one gets $\overline{\phi_h} + \phi_h' \equiv 0$. The third equation of (2.14) however states (after some simple computations) that $\overline{\phi_h'} = 0$, such that integrating in z the equation $\overline{\phi_h} + \phi_h' \equiv 0$ yields immediately $(\overline{\phi_h}, \phi_h') \equiv (0,0)$ and we have finished the proof. □

2.3.2 Comparison of the different AP-discretization matrices

In the equation (2.16b), A, denoted in the sequel by $\mathcal{M}_1$, is the matrix associated with the singular perturbation model, discretized by the finite element method introduced above. The matrix associated with the equation (2.16b), providing the fluctuating part and the Lagrangian approximation in the iterative resolution, will be denoted by $\mathcal{M}_2$. Finally we introduce $\mathcal{M}_3$ as the matrix associated with the solution of the whole system (2.15) providing the discrete approximations $(\phi_h', \bar{\phi}_h, \bar{P}_h)$. The structures and the sizes of these matrices are displayed in Figure 1. For completeness, the matrix associated with the original AP scheme (2.4),(2.6), denoted by $\mathcal{M}_O$, is also included in this comparison.

The matrix $\mathcal{M}_2$ is easily constructed thanks to the matrix of the singular perturbation problem by adding the two blocks related to the Lagrangian multiplier, corresponding to the zero-mean constraint. The discretization of this fluctuation equation is thus straightforward, requiring small localized modifications of the code providing the singular perturbation problem. The matrix $\mathcal{M}_O$ derived from the original AP scheme has the same size as $\mathcal{M}_2$ but with a significantly larger number of non-zero coefficients. This is easily explained by the contribution of the integro-differential operator in the left hand side of the fluctuation equation in (2.6). In the new AP-formulation this operator is moved to the right hand side providing a more sparse linear system. This underlines the essential advantages of the new AP-formulation introduced in this paper as compared to the one of [6]. Using the direct resolution increases the size of the linear system, since it provides the approximation for both components of the solution and for the Lagrangian. Note, however, that this increase of the matrix size is not dramatic, since both Lagrangian and mean part do not depend on z. The size of the blocks added in the matrix, namely B and C, is thus small compared with the size of A. Naturally both AP-formulations require the resolution of larger linear systems than the initial SP-model. However, the crucial advantage is that no additional numerical effort is needed to preserve the method accuracy when $\varepsilon \to 0$, which is not the case for the SP-model.

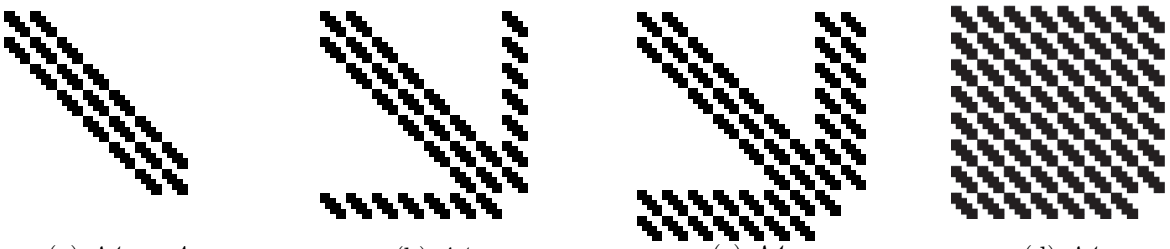

(a) $\mathcal{M}_1 = A$ (b) $\mathcal{M}_2$ (c) $\mathcal{M}_3$ (d) $\mathcal{M}_O$

Mat.	$\mathcal{M}_1 = A$	$\mathcal{M}_2 = \begin{pmatrix} A & B \\ B^T & 0 \end{pmatrix}$
Size	$N_x(N_z+2)$	$N_x(N_z+3)$
Nnz	$(3N_z+4)(3N_x-2)$	$(5N_z+8)(3N_x-2)$
Mat.	$\mathcal{M}_3 = \begin{pmatrix} A & \varepsilon C & B \\ \frac{1}{L_z}C^T & A_2 & 0 \\ B^T & 0 & 0 \end{pmatrix}$	$\mathcal{M}_O = \begin{pmatrix} \widetilde{A} & B \\ B^T & 0 \end{pmatrix}$
Size	$N_x(N_z+4)$	$N_x(N_z+3)$
Nnz	$(7N_z+13)(3N_x-2)$	$(N_z^2+6N_z+8)(3N_x-2)$

Figure 1: Structure (non-zero elements (Nnz)) and size of the discretization matrices for a grid size $(N_x, N_z) = (5, 5)$: (a) matrix associated with the singular perturbation problem (1.3), (b) matrix associated with the reformulated fluctuation equation(2.16b), (c) matrix associated with the direct resolution of the AP scheme (2.15), (d) matrix associated with the fluctuation equation of the original AP formulation (2.6).

To highlight the arguments stated above with some concrete examples, we compared in Table 1, for two example cases $(N_x, N_z) = (50, 50)$ resp. $(N_x, N_z) = (500, 500)$, the four different matrices $\mathcal{M}_1$, $\mathcal{M}_2$, $\mathcal{M}_3$ and $\mathcal{M}_O$. What can be observed is that the $\mathcal{M}_O$-matrix corresponding to the AP scheme of [6] is 11 times, even 101 times in the

500×500 case, more filled than the corresponding $\mathcal{M}_2$-matrix. This is rather drastic and underlines the advantages of the here introduced AP scheme as compared to the previous one. Interesting to observe is also that the ratio between matrix $\mathcal{M}_1$ and matrix $\mathcal{M}_2$ resp. between matrix $\mathcal{M}_1$ and matrix $\mathcal{M}_3$ is almost independent of the mesh size, which means that the numerical efforts in solving the SP-model or the AP-formulation remain similar.

		$\mathcal{M}_1$	$\mathcal{M}_O$	$\mathcal{M}_2$	$\mathcal{M}_3$
		SP-model	Original AP	Iterative AP	Direct AP
50×50	$p_1(\mathcal{M})$	0.34%	5.92%	0.54%	0.74%
	$p_2(\mathcal{M})$	1	18.2338	1.6753	2.3571
500×500	$p_1(\mathcal{M})$	0.00358%	0.6%	0.00594%	0.00829%
	$p_2(\mathcal{M})$	1	168.2234	1.6676	2.3358

Table 1: Number of non-zero elements (Nnz) in the linear systems associated with the SP problem, the original AP scheme, and both the iterative and direct new AP schemes, *i.e.* $p_1(\mathcal{M}) = \text{Nnz}(\mathcal{M})/\text{rk}(\mathcal{M})^2$, $p_2(\mathcal{M}) = \text{Nnz}(\mathcal{M})/\text{Nnz}(\mathcal{M}_1)$ where $\mathcal{M}$ is $\mathcal{M}_1$, $\mathcal{M}_O$, $\mathcal{M}_2$ and $\mathcal{M}_3$ respectively and $\text{rk}(\mathcal{M})$ denotes the rank of matrix $\mathcal{M}$.

2.3.3 Numerical investigation of the new AP formulation

In this subsection the new AP-formulation (2.12) of the singular perturbation problem (1.3) is studied. In particular, we wish to demonstrate that the new formulation provides the same properties as the original one [6], however with some major advantages. To this end, the numerical experiment proposed in [6] is reproduced. It consists in manufacturing an analytical set up for the problem, with an exact solution denoted ϕ_e and defined as

$$\phi_e(x,z) := \sin\left(\frac{2\pi}{L_x}x\right)\left(1+\varepsilon\cos\left(\frac{2\pi}{L_z}z\right)\right). \tag{2.17}$$

The coefficients of the elliptic problem (1.3) (verifying hypothesis 1) are defined as follows $A_\perp(x,z) = c_1 + xz^2$, $A_z(x,z) = c_2 + xz$, with two constants $c_1 > 0$, $c_2 > 0$. The right-hand side of the problem, denoted f, is analytically computed by injecting the exact solution ϕ_e into (1.3). An approximation of this function ϕ_h can then be computed thanks to the different numerical methods introduced above, their precision being analyzed thanks to the relative error

$$\|\phi_e - \phi_h\|_r = \frac{\|\phi_e - \phi_h\|_2}{\|\phi_e\|_2}. \tag{2.18}$$

Note that $\|\phi_e\|_2^2 = \frac{1}{2}(1+\frac{\varepsilon^2}{2})LxLz$, thus this norm does not vanish when $\varepsilon \to 0$. For these experiments the simulation domain $[0,1]\times[0,1]$ is discretized by a uniform mesh with either 50×50, 250×250 or 500×500 points, a $\mathbb{Q}_1$-finite element method and a three-point Gauss-Legendre quadrature formula for the integral-discretizations.

In Figure 2 the accuracy of the singular perturbation model (1.3), the New AP-formulation (2.4),(2.5) and the limit problem (1.5) are compared. For the AP scheme both resolutions (the iterative (2.16) and the direct (2.15) ones) are considered.

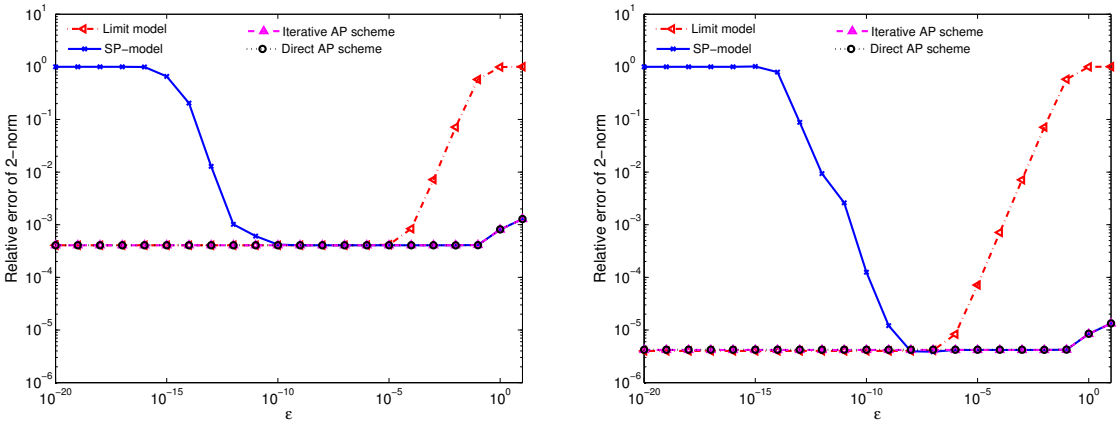

(a) (b)

Figure 2: Relative errors between the exact solution and its approximations computed via the L-model (1.5), the original SP model (1.3) as well as the iterative (2.16) and the direct new AP schemes (2.15) for (a): 50×50 and (b): 500×500 nodes.

One can observe that the limit model provides accurate approximations only for small values of the anisotropy ratio ε. For large enough ε-values the fluctuating part can not be neglected and a more complete model has to be used. The singular perturbation model provides accurate results only for large ε-values, the precision of the approximation deteriorates significantly for ε smaller than 10^{-10} on the coarsest grid (see Figure 2(a)). The domain of validity (accuracy) of the SP-model becomes even smaller on the refined mesh (see Figure 2(b)), that is because the condition number of the refined mesh problem is larger than that of the coarser grid problem. For example, when $\varepsilon = 10^{-12}$, the condition number for mesh 50×50 is estimated to be equal to 3.6387×10^{15}, this estimate being 3.3079×10^{17} for mesh 500×500. The accuracy of the solution, computed by the AP scheme, is almost ε-independent demonstrating thus the efficiency of this new AP formulation for all anisotropy strength.

The condition number of the different linear systems is plotted in Figure 3(a), as a function of ε. It is computed thanks to the block algorithm for matrix 1-norm estimation [9]. The new AP scheme provides the same advantageous features as the original scheme, with a matrix whose condition number is almost independent of the ε-values for large anisotropy ratios. The discretized singular perturbation problem gives a matrix whose condition number blows up with vanishing ε. This explains the poor accuracy of this scheme for large anisotropy ratios.

The computational efficiency, as a function of the anisotropy ratio, is evaluated in Table 3(b) for the different approaches. The time required for the computation via the singular perturbation model is used as a reference. This computations are performed thanks to a direct sparse linear solver PARDISO [19], [20] and do not depend on the ε-values (and consequently on the linear system conditioning). For the direct resolution, the linear system is solved only one time. While for the iterative resolution, two (different size) linear systems are solved several times until the difference between two successive solutions of system (2.16) is small enough. In particular, the L^∞-norm between two

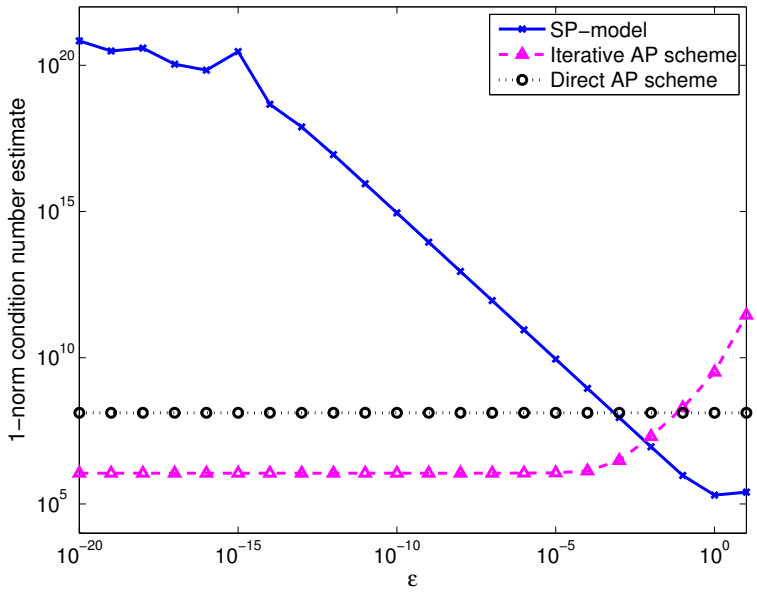

(a)

ε		1	10^{-1}	10^{-2}	10^{-3}	10^{-4}	10^{-5}	10^{-6}	10^{-7}	10^{-8}	10^{-9}	10^{-20}
Dire.	r_D	1.8	1.8	1.8	1.8	1.8	1.8	1.8	1.8	1.8	1.8	1.8
Iter.	r_I	6.0	5.4	5.0	4.0	3.4	2.2	2.0	2.0	1.7	1.7	1.7
	n_I	18	16	14	11	8	4	3	3	2	2	2

(b)

Figure 3: Comparison between the SP model (1.3), the iterative AP scheme (2.16) and the direct AP scheme (2.15) with a mesh size of 250 × 250. (a) Condition number estimate for the discretization matrices; (b) Computational time of the direct AP- resp. iterative AP-resolutions, divided by the computational time of the SP-model resolution, denoted by r_D, r_I respectively. The iteration number of iterative resolution, denoted by n_I, is also quoted. The linear systems are solved by the direct sparse solver PARDISO.

successive iterations (of the mean as well as fluctuation part) has to be inferior to the threshold value of 10^{-4}. Note that the most expensive part of the direct sparse linear solver is the matrix factorization. Thus in the iterative procedure we can store the factorized matrices, and use then these matrices in each iteration. Therefore we save a lot of computational time.

A larger number of non zeros elements as well as an increased system size explains the larger amount of computations required by the AP scheme. The direct resolution is roughly 80% slower than that of the SP-model. However, since the AP-reformulations provide matrices with a better conditioning, we expect the AP scheme to be more efficient than the SP-model when an iterative method is used as linear system solvers. Moreover, we note the efficiency of the iterative resolution. For the smallest ε-values its efficiency is comparable to that of the direct resolution. For the largest values, this approach is revealed to be computationally more demanding, due to a large number of iterations required to reach the convergence. For $\varepsilon = 1$, 18 iterations are indeed

necessary to compute an accurate approximation, giving rise to a computational effort almost three times as large as that of the direct resolution. However, these conclusions are closely related to the direct solver used for this investigations. More efficient linear system solver should be considered at this point (preconditioned Krylov subspace methods (see for instance [18, 3],[4]) or multigrid methods [1, 15]). However this is out of the scope of the present paper, which focuses on the introduction of an AP-scheme with sparse matrices.

3 Generalization to heterogeneous anisotropy ratios

In real physical situations the anisotropy ratio is not constant in the whole domain, and can even undergo huge variations. In order to address these problems, we adapt now the former AP-method to handle with variable anisotropy ratios.

3.1 Refitting of the AP-scheme

From now on, ε is a function of the coordinates (x, z), describing thus the variable anisotropy intensities. After the decomposition of the unknown in mean and average parts, the coupled system writes (for comparison see (2.4),(2.5))

$$\begin{cases} -\frac{\partial}{\partial x}\left(\overline{A_\perp}\frac{\partial \bar{\phi}}{\partial x}\right) = \bar{f} + \frac{\partial}{\partial x}\left(\overline{A_\perp \frac{\partial \phi'}{\partial x}}\right), & \text{in } \Omega_x, \\ \bar{\phi} = 0, & \text{on } \partial\Omega_x. \end{cases} \tag{3.1a}$$

$$\begin{cases} -\frac{\partial}{\partial x}\left(A_\perp \frac{\partial \phi'}{\partial x}\right) - \frac{\partial}{\partial z}\left(\frac{A_z}{\varepsilon}\frac{\partial \phi'}{\partial z}\right) = f + \frac{\partial}{\partial x}\left(A_\perp \frac{\partial \bar{\phi}}{\partial x}\right), & \text{in } \Omega, \\ \phi' = 0, & \text{on } \partial\Omega_x \times \Omega_z, \\ \partial_z \phi' = 0, & \text{on } \Omega_x \times \partial\Omega_z, \\ \overline{\phi'} = 0, & \text{in } \Omega_x. \end{cases} \tag{3.1b}$$

The average equation (3.1a) is the one derived for the homogeneous ε-case, the fluctuation equation (3.1b) being slightly modified. We introduce the same Hilbert-spaces $\mathbb{V}$, $\mathbb{W}$, as defined in section 2.1, and a new ε-independent scalar product

$$(\phi, \psi)_{\mathbb{V}} = (\partial_x \phi, \partial_x \psi)_{L^2(\Omega)} + (\partial_z \phi, \partial_z \psi)_{L^2(\Omega)}.$$

By redefining some terms of the bilinear forms (2.8), especially $a_0(\cdot,\cdot)$, $a(\cdot,\cdot)$ and $b(\cdot,\cdot)$

$$\begin{aligned}
a_0(\phi',\psi') &:= \int_0^{L_z}\int_0^{L_x} \frac{A_z(x,z)}{\varepsilon(x,z)}\frac{\partial\phi'}{\partial z}(x,z)\frac{\partial\psi'}{\partial z}(x,z)dxdz,\\
a_1(\phi',\psi') &:= \int_0^{L_z}\int_0^{L_x} A_\perp(x,z)\frac{\partial\phi'}{\partial x}(x,z)\frac{\partial\psi'}{\partial x}(x,z)dxdz,\\
a_2(\bar\phi,\bar\psi) &:= \int_0^{L_x} \bar A_\perp(x)\frac{\partial\bar\phi}{\partial x}(x)\frac{\partial\bar\psi}{\partial x}(x)dx,\\
a(\phi',\psi') &:= a_0(\phi',\psi') + a_1(\phi',\psi'),\\
b_1(\bar P,\psi') &:= \int_0^{L_x}\bar P(x)\int_0^{L_z}\frac{1}{\varepsilon(x,z)}\psi'(x,z)dzdx,\\
b_2(\phi',\bar Q) &:= \frac{1}{L_z}\int_0^{L_x}\bar Q(x)\int_0^{L_z}\phi'(x,z)dzdx,\\
c(\bar\phi,\psi') &:= \int_0^{L_z}\int_0^{L_x} A_\perp(x,z)\frac{\partial\bar\phi}{\partial x}(x)\frac{\partial\psi'}{\partial x}(x,z)dxdz,
\end{aligned} \tag{3.2}$$

the weak formulation of (3.1) writes now

$$\begin{cases} a_2(\bar\phi,\bar\psi) = (\bar f,\bar\psi) - \frac{1}{L_z}c(\bar\psi,\phi'), & \forall\bar\psi\in\mathbb{W},\\ a(\phi',\psi') = (f,\psi') - c(\bar\phi,\psi'), & \forall\psi'\in\mathbb{V}. \end{cases} \tag{3.3}$$

The AP-formulation of problem (3.3) is again deduced by introducing a Lagrange multiplier $\bar P$, corresponding to the constraint $\bar\phi'\equiv 0$. We thus have

$$(\mathrm{AP})_{var}\begin{cases} a_2(\bar\phi,\bar\psi) = (\bar f,\bar\psi) - \frac{1}{L_z}c(\bar\psi,\phi'), & \forall\bar\psi\in\mathbb{W},\\ a(\phi',\psi') + b_1(\bar P,\psi') = (f,\psi') - c(\bar\phi,\psi'), & \forall\psi'\in\mathbb{V},\\ b_2(\bar Q,\phi') = 0, & \forall\bar Q\in L^2(\Omega_x). \end{cases} \tag{3.4}$$

We shall now prove that the system (3.4) is equivalent to the problem (3.3).

Hypothesis 3. *Let in the following $\varepsilon\in L^\infty(\Omega)$, satisfying $0<\varepsilon_0\le\varepsilon(x,z)\le\varepsilon_M\le 1$ with ε_0 resp. ε_M two constants.*

Proposition 3.1. *Under hypothesis 1 and hypothesis 3, there exists a unique $(\bar\phi,\phi',\bar P)\in\mathbb{W}\times\mathbb{V}\times L^2(\Omega_x)$ satisfying (3.4). Moreover, the pair $(\bar\phi,\phi')$ is the unique solution of (3.3) and $\bar P\equiv 0$.*

Proof. The well-posedness of system (3.3) can be proved as we did in the constant ε-case. So it remains to prove the equivalence between the system (3.3) and system (3.4). First let $(\bar\phi,\phi')\in\mathbb{W}\times\mathbb{V}$ be the unique solution of system (3.3), then $(\bar\phi,\phi',0)$ will satisfy system (3.4). Inversely, we assume $(\bar\phi,\phi',\bar P)\in\mathbb{W}\times\mathbb{V}\times L^2(\Omega_x)$ to be a solution of system (3.4). Taking in the second equation of system (3.4), test functions ψ' depending only on x, leads to

$$\begin{aligned}
& L_z\int_0^{L_x}\overline{A_\perp\partial_x\phi'}\partial_x\psi'dx + \int_0^{L_x}\bar P(x)\psi'(x)\int_0^{L_z}\frac{1}{\varepsilon(x,z)}\,dz\,dx\\
=\ & L_z\int_0^{L_x}\bar f\psi'dx - L_z\int_0^{L_x}\overline{A}_\perp\partial_x\bar\phi\partial_x\psi'dx.
\end{aligned}$$

It is easy to see that $L_z \int_0^{L_x} \overline{A_\perp \partial_x \phi'} \partial_x \psi' dx + L_z \int_0^{L_x} \overline{A}_\perp \partial_x \bar{\phi} \partial_x \psi' dx = L_z \int_0^{L_x} \bar{f} \psi' dx$ according to the first equation of system (3.4). Thus we get

$$\int_0^{L_x} \bar{P}(x)\, \psi'(x) \int_0^{L_z} \frac{1}{\varepsilon(x,z)}\, dz\, dx = 0, \ \forall \psi' \in \mathbb{W}\,.$$

As $\int_0^{L_z} \frac{1}{\varepsilon(x,z)} dz > 0$, we deduce that $\bar{P} \equiv 0$, by density arguments. □

3.2 Steep gradients of the heterogeneous anisotropy ratio

Before discretizing the AP-formulation (3.4), we first have to think about the numerical problems arising from rapid variations of the function $\frac{1}{\varepsilon}$, especially for the numerical integration procedures. As we know, a rapidly varying continuous function can be considered numerically as a discontinuous function in certain intervals of a grid. One can refine the discretization mesh to obtain a preciser approximate solution, but with more computational efforts. To overcome this difficulty of discretizing abrupt gradients, let us thus propose here three approaches which are more detailed in appendix A. We shall consider, for the sake of simplicity, anisotropies $\varepsilon(z)$ depending only on z.
The first approach is to use a non-conservative formulation for the fluctuation equation. By developing $\frac{\partial}{\partial z}\left(\frac{A_z}{\varepsilon}\frac{\partial \phi'}{\partial z}\right)$ in (3.1b), we obtain the following equation

$$-\varepsilon \frac{\partial}{\partial x}\left(A_\perp \frac{\partial \phi'}{\partial x}\right) - \frac{\partial}{\partial z}\left(A_z \frac{\partial \phi'}{\partial z}\right) + \frac{\partial(\ln \varepsilon)}{\partial z} A_z \frac{\partial \phi'}{\partial z} = \varepsilon f + \varepsilon \frac{\partial}{\partial x}\left(A_\perp \frac{\partial \bar{\phi}}{\partial x}\right).$$

To implement this approach, we use again the bilinear forms (2.8), but change only $a(\phi', \psi')$ in

$$a_0(\phi', \psi') := \int_0^{L_z} \int_0^{L_x} A_z(x,z) \frac{\partial \phi'}{\partial z}(x,z) \frac{\partial \psi'}{\partial z}(x,z) + \frac{\partial \ln \varepsilon(z)}{\partial z} A_z(x,z) \frac{\partial \phi'}{\partial z}(x,z) \psi'(x,z) dx dz.$$

However, this expression is no longer in a conservative form.

Secondly, we use the harmonic mean method detailed in section A.3. The third approach is the Scharfetter-Gummel scheme given in section A.4. In the sequel we investigate the efficiency of these AP-formulations for anisotropy ratios with large gradients.

3.3 Numerical results

To verify the efficiency of the AP scheme for highly heterogeneous anisotropy ratio problems, we choose an artificially constructed variable ε test case. We use again the exact solution and the diffusion matrix of the constant ε case, but replace the constant ε by a variable one, of the form

$$\varepsilon(z) = \begin{cases} \frac{1}{2}\left(\varepsilon_{\max}\left(1 + \tanh\left(q\left(0.1L_z - z\right)\right)\right) + \varepsilon_{\min}\left(1 - \tanh\left(q\left(0.1L_z - z\right)\right)\right)\right), \\ \qquad\qquad \text{if } 0 \le z \le \frac{L_z}{2}, \\ \frac{1}{2}\left(\varepsilon_{\max}\left(1 + \tanh\left(q\left(z - 0.9L_z\right)\right)\right) + \varepsilon_{\min}\left(1 - \tanh\left(q\left(z - 0.9L_z\right)\right)\right)\right), \\ \qquad\qquad \text{if } \frac{L_z}{2} \le z \le L_z. \end{cases} \tag{3.5}$$

The variable ε is controlled by three parameters q, $\varepsilon_{\max}$, $\varepsilon_{\min}$: q describes the steep slope of the curve, $\varepsilon_{\max}$, $\varepsilon_{\min}$ control the maximum and minimum values of ε. An example of $\varepsilon(z)$ is illustrated in Figure 4.

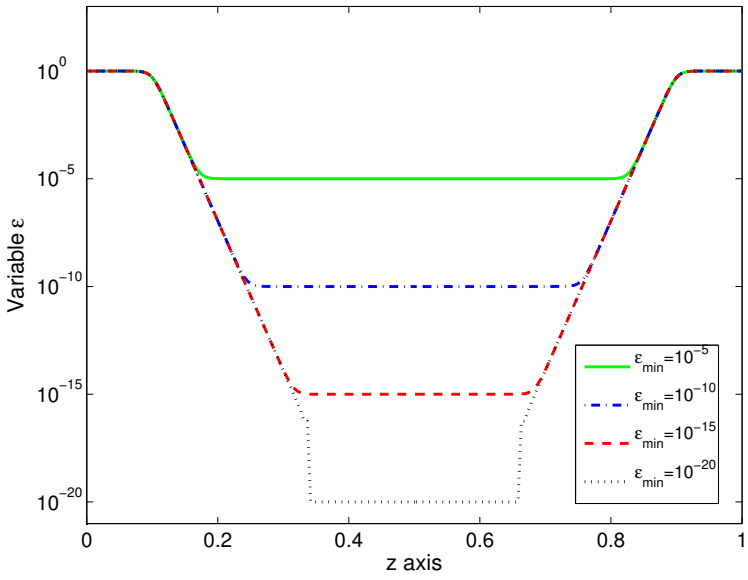

Figure 4: Profile of the anisotropy ratio reciprocal ε as defined by equation (3.5) for $\varepsilon_{\max} = 1$, $q = 80$ and $\varepsilon_{\min}$ equal to 10^{-5}, 10^{-10}, 10^{-15}, 10^{-20}.

In the following numerical tests, we fix the parameters $\varepsilon_{\max} = 1$, $q = 80$ and vary the parameter $\varepsilon_{\min}$ from 10^{-20} to 1. The right-hand side f is obtained by injecting $\phi_e(x, z)$ into equation (1.3). We shall compare the numerical results obtained by all the methods mentioned above: 2D SP-model (1.3) discretized by the $\mathbb{Q}_1$ finite element method, the standard AP scheme (3.4), the non-conservative AP scheme, the harmonic mean AP scheme, and the Scharfetter-Gummel AP scheme.

In Figure 5(a), we observe that the relative error in the L^2-norm of the SP-model increases with vanishing $\varepsilon_{\min}$ values. This error remains close to 10^{-3} for $\varepsilon_{\min}$ between 10^{-3} and 10^{-11}, but blows up for $\varepsilon_{\min} \leq 10^{-11}$. The curve of the standard AP scheme coincides with that of the SP-model when $\varepsilon_{\min} > 10^{-11}$, the accuracy of the former one remaining $\varepsilon_{\min}$ independent for larger anisotropy ratios. The non-conservative AP scheme demonstrates a non monotone accuracy evolution, with a peak obtained for $\varepsilon_{\min} = 10^{-2}$. However, the error norm is close to 2×10^{-4} for $\varepsilon_{\min}$ below 10^{-5}. The curve of the harmonic mean AP scheme is similar to that of the standard AP scheme but with smaller relative error. Finally, the Scharfetter-Gummel AP scheme gives the best accuracy with a relative error of one order smaller than that of the standard AP scheme.

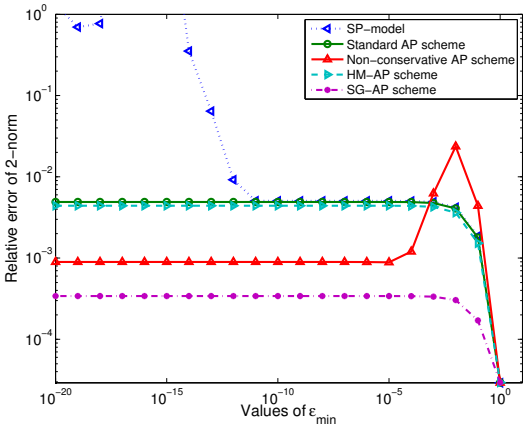

(a) Relative error between the exact solution and its approximations, as a function of $\varepsilon_{\min}$

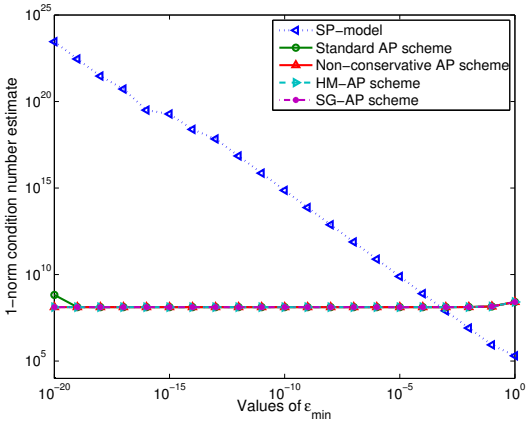

(b) Condition number estimate of the equilibrated matrices, as a function of $\varepsilon_{\min}$

Figure 5: Comparison of the SP-model, the standard AP scheme, the non-conservative AP scheme, the harmonic mean AP scheme (HM-AP) and the Scharfetter-Gummel AP scheme (SG-AP) for 2D computations carried out on a 250×250 mesh.

In Figure 5(b) the condition number estimates of the different methods are displayed. These estimates are computed after an equilibration of the matrices is performed. This procedure consists in multiplying $\mathcal{M}_2$, respectively $\mathcal{M}_3$, by the row balance matrix $\mathcal{P}_2$, respectively $\mathcal{P}_3$, defined as

$$\mathcal{P}_2 = \begin{pmatrix} \mathcal{E}_0 & & & \\ & \ddots & & \\ & & \mathcal{E}_{N_z+1} & \\ & & & I \end{pmatrix}, \qquad \mathcal{P}_3 = \begin{pmatrix} \mathcal{E}_0 & & & \\ & \ddots & & \\ & & \mathcal{E}_{N_z+1} & \\ & & & I \\ & & & & I \end{pmatrix},$$

where $\mathcal{E}_k = \varepsilon(z_k)I$ for $0 \leq k \leq N_z + 1$ and I is the $N_x \times N_x$ identity matrix. As in the homogeneous ε case, the condition number of the SP-model increases with the anisotropy ratio, while the curves corresponding to the four AP schemes almost coincide and remain quite independent of the $\varepsilon_{\min}$ values.

4 Conclusion

In this paper, we introduced a new Asymptotic-Preserving formulation for a highly anisotropic elliptic equation and compared it with the AP scheme proposed initially in [6]. The new AP scheme is based again on a decomposition of the unknown in its mean part and its fluctuating part, but the fluctuation equation is different. The discretization matrix associated to this new AP-formulation is much more sparse than that of the original one, establishing thus the significant efficiency of this new method. The AP-property of the scheme is also investigated, in particular the well-posedness in the limit $\varepsilon \to 0$. Finally we consider highly heterogeneous anisotropy ratio problems, in view of real physical applications.

A 1D simulations for heterogeneous anisotropy ratios with steep gradients

In this section, we detail different procedures to deal with huge variations in the anisotropy intensities. A slightly modified 1D framework is investigated in order to simplify the presentation of the different approaches used in section 3.3 for the 2D simulations. The 1-dimensional SP-model now reads

$$\begin{cases} -\frac{\mathsf{d}}{\mathsf{d}z}\left(\frac{1}{\varepsilon(z)}\frac{\mathsf{d}u}{\mathsf{d}z}\right) + u = f, & \text{in } \Omega_z, \\ \frac{\mathsf{d}}{\mathsf{d}z}u = 0, & \text{on } \partial\Omega_z. \end{cases} \tag{A.1}$$

where u is the unknown of the problem, ε is a positive function of z and $\Omega_z = [0, L_z]$. Note that the equation (A.1) is well-posed for $\varepsilon(z) > 0$. The uniqueness of the solution is the 1D case is achieved by adding a term in the equation. This was not needed in the 2D case, due to the presence the derivative in the second direction x. Taking now $\varepsilon(z) := \delta\chi(z)$ and passing to the limit $\delta \to 0$, yields the degenerate problem

$$\begin{cases} -\frac{\mathsf{d}}{\mathsf{d}z}\left(\frac{1}{\chi(z)}\frac{\mathsf{d}u}{\mathsf{d}z}\right) = 0, & \text{in } \Omega_z, \\ \frac{\mathsf{d}}{\mathsf{d}z}u = 0, & \text{on } \partial\Omega_z, \end{cases} \tag{A.2}$$

which is ill-posed, since all constants are solutions.

A standard AP-discretization is compared with a non conservative AP-scheme as well as a Harmonic-Mean and a Scharfetter-Gummel AP-scheme.

A.1 The standard AP-scheme

To construct the AP-scheme corresponding to this SP-model, let us decompose u into its mean part $\bar{u}$ and its fluctuating part u' and follow the guideline of section 2.1. By integrating equation (A.1) in Ω_z, we get the average equation $\bar{u} = \bar{f}$. Subtracting this equation from (A.1) and introducing the Lagrange multiplier λ, we obtain the following AP-formulation

$$\begin{cases} \bar{u} = \bar{f}, \\ \displaystyle\int_0^{L_z} \left[\frac{1}{\varepsilon(z)}\frac{\mathsf{d}u'}{\mathsf{d}z}\frac{\mathsf{d}v'}{\mathsf{d}z} + u'v'\right]\mathsf{d}z + \lambda\int_0^{L_z}\frac{1}{\varepsilon(z)}v'\mathsf{d}z = \\ \qquad\qquad \displaystyle\int_0^{L_z} f'v'\mathsf{d}z, \quad \forall v' \in H^1(\Omega_z), \\ \displaystyle\int_0^{L_z} u'\mathsf{d}z = 0. \end{cases} \tag{A.3}$$

This AP scheme will be discretized by a $\mathbb{P}_1$ finite element method. However, note that the difficulty here is the approximation of the high anisotropy-gradients. To face this problem, we shall propose here different methods.

A.2 Non-Conservative AP-scheme

In this approach, we try to circumvent the high anisotropy ratio term $\frac{1}{\varepsilon}$ in the fluctuation equation of (A.3). This is done, by developing $\frac{\mathsf{d}}{\mathsf{d}z}\left(\frac{1}{\varepsilon(z)}\frac{\mathsf{d}u'}{\mathsf{d}z}\right)$, in order to obtain

$$\frac{\mathsf{d}}{\mathsf{d}z}\left(\ln\varepsilon(z)\right)\frac{\mathsf{d}u'}{\mathsf{d}z}-\frac{\mathsf{d}^2u'}{\mathsf{d}z^2}+\varepsilon u'=\varepsilon f'. \tag{A.4}$$

By injecting (A.4) in the AP-reformulation, we get another reformulation, *i.e.*

$$\begin{cases} \bar{u}=\bar{f}, \\ \displaystyle\int_0^{L_z}\left[\frac{\mathsf{d}}{\mathsf{d}z}\left(\ln\varepsilon(z)\right)\frac{\mathsf{d}u'}{\mathsf{d}z}v'+\frac{\mathsf{d}u'}{\mathsf{d}z}\frac{\mathsf{d}v'}{\mathsf{d}z}+\varepsilon u'v'\right]\mathsf{d}z+\lambda\int_0^{L_z}v'\mathsf{d}z \\ \qquad\qquad =\displaystyle\int_0^{L_z}\varepsilon f'v'\mathsf{d}z,\quad \forall v'\in H^1(\Omega_z), \\ \displaystyle\int_0^{L_z}u'\mathsf{d}z=0. \end{cases} \tag{A.5}$$

Again, we shall discretize (A.5) by the $\mathbb{P}_1$ finite element method.

A.3 Harmonic Mean AP-scheme

The harmonic mean AP scheme is just a special discretization of the AP-formulation (A.3) following the ideas detailed in [21, 23]. To present this approach, let us again consider the partition of Ω_z and the basis functions defined in section 2.3.1. Taking now in (A.3) as test functions $\kappa_k(z)$ and replacing $u'(z)$ by $\displaystyle\sum_{l=0}^{N_z+1}\alpha_l\kappa_l(z)$ give rise for $k=1,\cdots,N_z$ to

$$\begin{aligned} &-\frac{p_k}{\Delta z^2}\alpha_{k-1}+\left(\frac{p_k}{\Delta z^2}+\frac{p_{k+1}}{\Delta z^2}\right)\alpha_k-\frac{p_{k+1}}{\Delta z^2}\alpha_{k+1} \\ &\quad+\sum_{l=k-1}^{k+1}\alpha_l\int_{z_{k-1}}^{z_{k+1}}\kappa_l(z)\kappa_k(z)\mathsf{d}z+q_k\lambda=f_k, \end{aligned}$$

where $p_k=\displaystyle\int_{z_{k-1}}^{z_k}\frac{1}{\varepsilon(z)}\mathsf{d}z$, $q_k=\displaystyle\int_{z_{k-1}}^{z_{k+1}}\frac{1}{\varepsilon(z)}\kappa_k(z)\mathsf{d}z$, $f_k=\displaystyle\int_{z_{k-1}}^{z_{k+1}}f'(z)\kappa_k(z)\mathsf{d}z$. If we discretize p_k by a standard numerical quadrature formula, the obtained scheme will just be a $\mathbb{P}_1$ finite element method. However, we will use instead a harmonic mean to approximate p_k, *i.e.*

$$p_k\approx\Delta z^2\left(\int_{z_{k-1}}^{z_k}\varepsilon(z)\mathsf{d}z\right)^{-1}.$$

Finally, the integration $\displaystyle\int_{z_{k-1}}^{z_k}\varepsilon(z)\mathsf{d}z$ is approximated by a standard numerical quadrature, for example Gauss-Legendre quadrature. By this manner, we obtain the full harmonic mean AP scheme.

A.4 Scharfetter-Gummel AP-scheme

The Scharfetter-Gummel AP-scheme is an amelioration of the harmonic mean AP-scheme. In particular a special quadrature formulae is used to approximate p_k [21]. Denoting $\varepsilon(z_k)$ simply by ε_k, we approximate p_k as follows

- if $\varepsilon_{k-1} \neq \varepsilon_k$,

$$\begin{aligned} p_k &\approx \Delta z^2 \left(\int_{z_{k-1}}^{z_k} \varepsilon(z) \mathsf{d}z \right)^{-1} = \Delta z^2 \left(\int_{z_{k-1}}^{z_k} e^{\ln \varepsilon(z)} \mathsf{d}z \right)^{-1} = \Delta z^2 \left(\int_{z_{k-1}}^{z_k} \frac{\mathsf{d}e^{\ln \varepsilon(z)}}{\mathsf{d}\ln \varepsilon(z)} \mathsf{d}z \right)^{-1} \\ &\approx \Delta z^2 \left(\Delta z \frac{e^{\ln \varepsilon_k} - e^{\ln \varepsilon_{k-1}}}{\ln \varepsilon_k - \ln \varepsilon_{k-1}} \right)^{-1} = \Delta z \frac{\ln \varepsilon_k - \ln \varepsilon_{k-1}}{\varepsilon_k - \varepsilon_{k-1}}, \end{aligned}$$

- if $\varepsilon_{k-1} = \varepsilon_k$,

$$p_k \approx \Delta z \frac{1}{\varepsilon_k}.$$

  where $\ln \varepsilon$ is approximated by $\sum_{k=0}^{N_z+1} \ln \varepsilon_k \kappa_k$.

A.5 Numerical results

To compare these approaches, we take an exact solution of equation (A.1) defined as

$$u_e(z) := \varepsilon(z) \cos\left(\frac{2\pi}{L_z} z \right), \tag{A.6}$$

with $\varepsilon(z)$ defined by expression (3.5). We shall compare the SP-model, the standard AP scheme, the Non-Conservative AP scheme, the Harmonic Mean AP scheme and the Scharfetter-Gummel AP scheme respectively. For this, we choose $q = 80$, $\varepsilon_{\max} = 1$ and different values for $\varepsilon_{\min}$. The relative error of the approximations with the exact solution are gathered in Figure 6. The results reported in the table 6(c) show that the SP-model can not furnish an accurate approximation of the solution. On the contrary the curves related to the approximation computed by the AP-schemes displayed on figure 6(a) and 6(b) demonstrate the robustness of these schemes. The standard AP-scheme as well as the HM-AP scheme appear to be rather unprecise in the region near the anisotropy steep gradients, while the NC-AP scheme exhibits oscillations in the same regions. Finally, the SG-AP scheme provides the best approximation above the different methods proposed.

References

[1] M. F. Adams, *Algebraic multigrid methods for constrained linear systems with applications to contact problems in solid mechanics*, Numer. Linear Algebra Appl., Vol 11, (2004), pp 141–153.

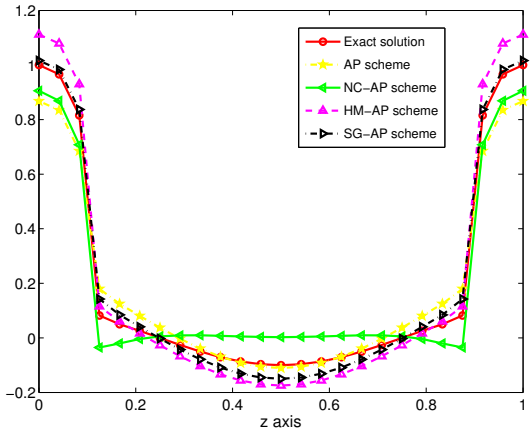

(a) $\varepsilon_{\min} = 10^{-1}$

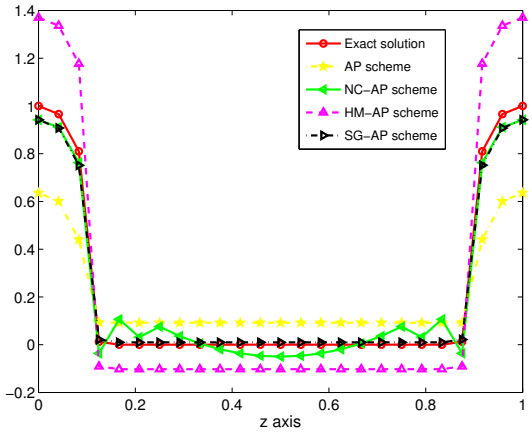

(b) $\varepsilon_{\min} = 10^{-10}$

$\varepsilon_{\min}$	SP-model	AP scheme	NC-AP scheme	HM-AP scheme	SG-AP scheme
10^{-1}	26.4022	0.1652	0.1486	0.1532	0.0734
10^{-10}	11.5878	0.4310	0.1171	0.4434	0.0653

(c) Relative errors between the exact solution and the approximate ones

Figure 6: Comparison between a standard discretization of the SP-model, the AP scheme, the non-conservative AP (NC-AP) scheme, the harmonic mean AP (HM-AP) scheme and the Scharfetter-Gummel AP (SG-AP) scheme on a grid with 25 points. (a) Plots of the approximate solutions computed thanks to the different methods for $\varepsilon_{\min} = 10^{-1}$; (b) Same plots for $\varepsilon_{\min} = 10^{-10}$; (c) Relative errors between the exact solution and the approximate ones for both cases $\varepsilon_{\min} = 10^{-1}$ and $\varepsilon_{\min} = 10^{-10}$.

[2] S. F. Ashby, R. D. Falgout, T. W. Fogwell, A. F. B. Tompson, *A numerical solution of groundwater flow and contaminant transport on the CRAY T3D and C90 supercomputers*, Int. J. High Perform. Comp. Appl., Vol. 13 (1999), pp 80–93.

[3] R. Barrett, M. Berry, T. F. Chan, J. Demmel, J. Donato, J. Dongarra, V. Eijkhout, R. Pozo, C. Romine and H. Van der Vorst , *Templates for the Solution of Linear Systems: Building Blocks for Iterative Methods*, SIAM, Philadelphia (19924).

[4] M. Benzi and A. J. Wathen, *Some Preconditioning Techniques for Saddle Point Problems*, in W. Schilders, H. A. van der Vorst and J. Rommes, eds., Model Order Reduction: Theory, Research Aspects and Applications, Springer-Verlag (Series: Mathematics in Industry), 2008, pp. 195-211.

[5] P. Degond, F. Deluzet, L. Navoret, A.-B. Sun, M.-H. Vignal, *Asymptotic-Preserving Particle-In-Cell method for the Vlasov-Poisson system near quasineutrality*, J. Comput. Phys, 229 (2010), pp 5630-5652.

[6] P. Degond, F. Deluzet, C. Negulescu, *An asymptotic preserving scheme for strongly anisotropic elliptic problems* , SIAM-MMS (Multiscale Modeling and Simulation), Vol. 8, No. 2 (2010), pp 645–666.

[7] P. Degond, A. Lozinki, J. Narski, C. Negulescu, *An asymptotic preserving method for highly anisotropic elliptic equations based on a micro-macro decomposition*, J. Comput. Phys, 231 (2012), pp. 2724–2740.

[8] John Keith Hargreaves. *The solar-terrestrial environment: an introduction to geospace–the science of the terrestrial upper atmosphere, ionosphere, and magnetosphere*. Cambridge University Press, 1992.

[9] N. J. Higham, F. Tisseur, *A Block Algorithm for Matrix 1-Norm Estimation, with an Application to 1-Norm Pseudospectra*, SIAM J. Matrix Anal. Appl. Vol. 21, No. 4 (2000), pp 1185–1201.

[10] T. Y. Hou, X. H. Wu, *A Multiscale Finite Element Method for Elliptic Problems in Composite Materials and Porous Media*, J. Comput Phys. , 134, (1997), pp 169–189.

[11] R. D. Hunsucker and J. K. Hargreaves. *The High-Latitude Ionosphere and its Effects on Radio Propagation*. Cambridge Atmospheric and Space Science Series. Cambridge University Press, 2002.

[12] S. Jin, *Efficient Asymptotic-Preserving (AP) schemes for some multiscale kinetic equations*, SIAM J. Sci. Comp., Vol. 21 (1999), pp 441–454.

[13] M. C. Kelley, W. E. Swartz, J.J. Makela, *Mid-Lattitude ionospheric fluctuation spectra due to secondary $E \times B$ instabilities*, J. Atmos. Solar-Terr. Phys., Vol. 66 (2004), pp 1559–1565.

[14] M. J. Keskinen, S. L. Ossakow, B. G. Fejer, *Three-dimensional nonlinear evolution of equatorial ionospheric spread-F bubbles*,Geophys. Res. Lett., Vol. 30 (2003), pp 41–44.

[15] P. Krzyzanowski, *A class of block smoothers for multigrid solution of saddle point problems with application to fluid flow*, Proceedings of PPAM'2003. pp 1006–1013.

[16] T. Manku, A. Nathan, *Electrical properties of silicon under nonuniform stress*, J. Appl. Phys. **74** (1993), pp 1832.

[17] Henry Rishbeth and Owen K. Garriott. *Introduction to ionospheric physics [by] Henry Rishbeth [and] Owen K. Garriott*. International geophysics series ; v. 14. Academic Press, New York,, 1969. Revision and expansion of Stanford Electronics Laboratories report SU-SEL-64-111 issued in 1964 under title: Introduction to the ionosphere and geomagnetism. Bibliography: p. 275-309.

[18] Y. Saad and M.H. Schultz, *GMRES: A Generalized Minimal Residual Algorithm for Solving Nonsymmetric Linear Systems*, SIAM J. Sci. Comp. , Vol. 7, No. 3 (1986), pp 856–859.

[19] O. Schenk and K. Gartner, *Solving Unsymmetric Sparse Systems of Linear Equations with PARDISO*, Journal of Future Generation Computer Systems, Vol. 20, No. 3 (2004), pp 475–487.

[20] O. Schenk, A. Waechter, and M. Hagemann, *Matching-based Preprocessing Algorithms to the Solution of Saddle-Point Problems in Large-Scale Nonconvex Interior-Point Optimization.* Journal of Computational Optimization and Applications, Vol. 36, No. 2-3(2007), pp 321–341.

[21] N. Saito, *An interpretation of the Scharfetter-Gummel finite difference scheme*, Proc. Japan Acad., Vol. 82, Ser. A (2006), pp 187–191.

[22] A.-M. Tréguier, *Modélisation numérique pour l'océanographie physique*, Ann. math. Blaise Pascal, tome 9, no. 2 (2002), pp 345–361.

[23] T. Tsuchiya, K.Yoshida and S. Ishioka, *Yamamoto's principle and its applications to precise finite element error analysis*, J.comput. Appl. Math. Vol. 152, No. 1-2 (2003), pp 507–532.

[24] W.-W. Wang, X.-C. Feng, *Anisotropic diffusion with nonlinear structure tensor*, Multiscale Model Sim., Vol. 7, no. 2 (2008), pp 963–977.

[25] J. Weickert, *Anisotropic Diffusion in Image Processing* , Teubner, Stuttgart, (1998).